Photon-number-discriminating detection using a quantum-dot, optically gated, field-effect transistor

E. J. GANSEN[1]*, M. A. ROWE[1], M. B. GREENE[1], D. ROSENBERG[2], T. E. HARVEY[1], M. Y. SU[1], R. H. HADFIELD[3], S. W. NAM[1] AND R. P. MIRIN[1]

[1]Optoelectronics Division, National Institute of Standards and Technology, Boulder, Colorado 80305, USA
[2]Los Alamos National Laboratory, Los Alamos, New Mexico 87545, USA
[3]Heriot-Watt University, Edinburgh EH14 4AS, UK
*e-mail: gansen@boulder.nist.gov

Published online: 1 October 2007; doi:10.1038/nphoton.2007.173

Detectors with the capability to directly measure the photon number of a pulse of light[1–3] enable linear optics quantum computing[4], affect the security of quantum communications[5], and can be used to characterize[6–8] and herald[9] non-classical states of light. Here, we demonstrate the photon-number-resolving capabilities of a quantum-dot, optically gated, field-effect transistor that uses quantum dots as optically addressable floating gates in a GaAs/$Al_{0.2}Ga_{0.8}As$ δ-doped field-effect transistor. When the active area of the detector is illuminated, photo-generated carriers trapped by quantum dots screen the gate field, causing a persistent change in the channel current that is proportional to the number of confined carriers. Using weak laser pulses, we show that discrete numbers of trapped carriers produce well resolved changes in the channel current. We demonstrate that for a mean photon number of 1.1, decision regions can be defined such that the field-effect transistor determines the number of detected photons with a probability of accuracy greater than 83%.

The composition and principles of operation of the quantum-dot, optically gated, field-effect transistor (QDOGFET) are shown in Fig. 1. The structure is specifically designed to efficiently detect photons absorbed in the active GaAs layer separating the quantum dots (QDs) and a two-dimensional electron gas (2DEG). When a reverse bias is applied to the gate, electrons and holes photo-excited in the absorption layer are separated by the internal electric field. The holes are directed towards the QDs, where they are trapped, while the electrons are swept in the opposite direction, where they join the 2DEG. Confined to the QDs, the positively charged holes screen the internal gate field. The effective increase of the gate bias is subsequently monitored as an increase in the current flowing in the 2DEG, as dictated by the transconductance, g_m, of the field-effect transistor (FET). It has been shown[10] that in the small-signal limit the increase in the channel current, I_{ds}, caused by the trapping of N photo-generated holes in the QD layer is given by

$$\Delta I_{ds} = g_m \frac{eW}{\varepsilon' A} N \qquad (1)$$

where e is the elementary charge, W is the distance between the Pt gate and the QD layer, ε' is the electric permittivity and A is the active area. Over time, the charging of the QDs caused by capture of even a single photo-generated hole results in a large change in the cumulative charge transferred in the 2DEG. The photoconductive gain[11] associated with this process provides the detector with single-photon sensitivity[12]. Moreover, because ΔI_{ds} is proportional to N, the channel response provides a direct measure of the number of detected photons. Previously, we investigated the photo-response of a bare QDOGFET (fabricated without an opaque Au aperture) under pulsed-laser illumination and demonstrated that, when averaged over many laser pulses, ΔI_{ds} increased linearly with N, in accordance with equation (1) (ref. 12). However, owing to secondary sources of photo-generated signals[12,13], the individual current changes produced by different numbers of photons were not well resolved. Similar photon-number dependent responses have also previously been observed from another QD-based detector, providing the device with some limited photon-number resolution[14]. In this work, we explicitly demonstrate the ability of our apertured QDOGFET to perform single-shot, photon-number-discriminating measurements. We construct histograms of the detector's responses to individual laser pulses that exhibit well-defined peaks associated with the detection of discrete numbers of photons. We show that the measured photon distributions obey Poisson statistics and use the data to quantify the fidelity of the detector.

Realizing the photon-number-resolving capabilities of the QDOGFET requires that each photo-generated hole trapped in a QD changes I_{ds} by an equal amount, regardless of the location of the charged QDs within the ensemble. This property of the device is implicit in the derivation of equation (1). It is also important that parasitic signals associated with the excitation of carriers in portions of the structure other than the dedicated absorption region do not contaminate the signal changes caused by the charging of QDs beneath the Pt gate. Our previous studies[12,13] of bare QDOGFET structures indicate that photons absorbed in the ungated portions of the channel mesa (near the edges of the active region) and absorbed in the GaAs buffer layer

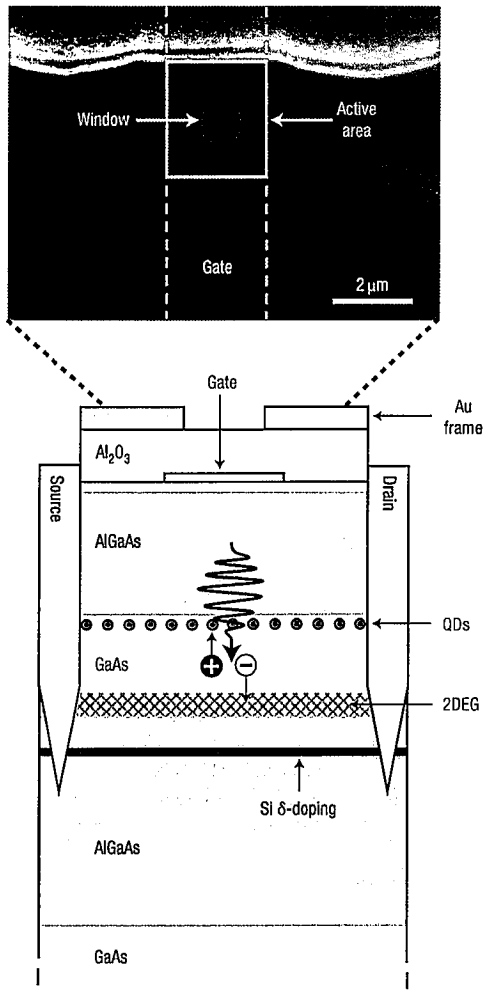

Figure 1 Diagram of a QDOGFET. Semiconductor layers (from bottom to top): GaAs substrate and 200 nm GaAs buffer layer, 2.5 μm $Al_{0.2}Ga_{0.8}As$, Si δ-doping ($\sim 1 \times 10^{12}$ cm^{-2}), 70 nm $Al_{0.2}Ga_{0.8}As$, 100 nm GaAs, InGaAs QDs (400–500 μm^{-2}), 200 nm $Al_{0.2}Ga_{0.8}As$,10 nm n-doped ($\sim 6 \times 10^{17}$ cm^{-3}) GaAs cap. The device was fabricated by etching a channel mesa between the Ni/Au/Ge source and drain ohmic contacts and by depositing a semitransparent Pt Schottky barrier gate midchannel. The gated portion of the channel mesa defines the active area (2.0 μm × 2.4 μm). Photo-absorption is limited to the interior of the active area by an opaque Au mask with a 0.7 μm × 0.7 μm transmission window. A ~100-nm-thick transparent layer of Al_2O_3 separates the Au frame from the rest of the structure. Layers are not drawn to scale. A scanning electron microscope image shows the top of the detector.

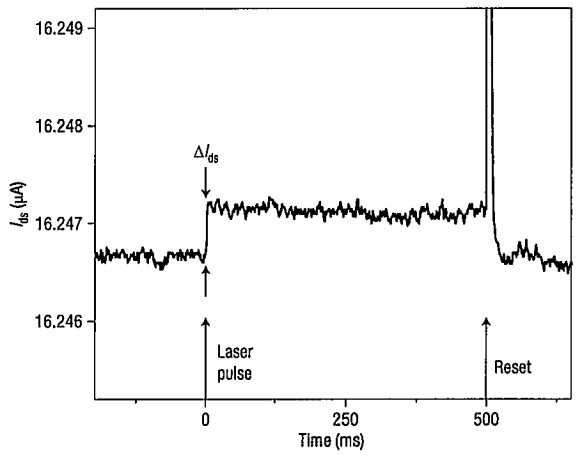

Figure 2 Persistent photo-response. Single-shot measurement of I_{ds} responding to a 20-μs laser pulse arriving at $t = 0$. During illumination, a reverse bias of −0.5 V was applied to the gate. The detector was electrically reset at $t = 500$ ms by raising the applied gate bias to +1 V for 10 ms.

contribute to the total photo-response of the detector. These contributions contaminate the signal changes caused by the charging of QDs within the active area of the device. By masking the gated area of the QDOGFET with an opaque Au aperture (shown in Fig. 1), we prevent the absorption of photons in the ungated portions of the channel and promote hole capture in QDs located within the interior of the active region, which are expected to produce the most uniform signal changes. In addition, we eliminate signal contributions from carriers excited in the GaAs buffer layer by electrically isolating the buffer layer from the ohmic contacts. This is accomplished by growing a sufficiently thick AlGaAs layer between the buffer layer and the δ-doping.

We investigated the ability of the QDOGFET to resolve the number of detected photons by illuminating the device with attenuated laser pulses and by constructing histograms of the current changes, ΔI_{ds}, produced by the individual pulses of light (typical response curve shown in Fig. 2). Figure 3 shows histograms obtained for five different average pulse fluences, where each panel is labelled with the mean number of photons detected per laser pulse, $\bar{N}$ (values extracted from numerical fits of the data, as described below). Given the geometry, material composition, and the measured transconductance of the QDOGFET used in these measurements, equation (1) predicts that each trapped hole should change I_{ds} by 0.19 nA. Grey vertical lines dictated by $\Delta I_{ds} = N \times 0.19$ nA are included in the figure. In the absence of laser light ($\bar{N} = 0$), the histogram consists of a single peak associated with the detection of zero photons, where the spread in the distribution represents current fluctuations associated with electrical noise. By comparison, when the device is weakly illuminated, additional peaks are apparent in the data. Distinct peaks centred around $\Delta I_{ds} = 0.19$ nA and 0.38 nA are observed, associated with the detection of $N = 1$ and 2 photons, respectively. Peaks associated with higher photon numbers ($N \geq 3$) are more difficult to distinguish in the data, suggesting that the resolution of the detector degrades with increasing photon number.

To quantitatively analyse the photon-number resolution of the QDOGFET, we fit each histogram shown in Fig. 3 with a series of five gaussian functions (shown as red dashed curves), accounting for the detection of 0, 1, 2, 3 and 4 photons. We constrained the fits such that the areas of the gaussian peaks obey Poisson statistics, with $\bar{N}$ defined as a free fit parameter. Within the statistical scatter in the data, the constrained numerical fits follow the measured histograms quite well. The individual gaussian functions are positioned at 0.20 ± 0.02 nA intervals over a dynamic range of three photons. To check self-consistency of the analysis, we evaluate $\mu/\bar{N}$ (μ is the distribution mean) for each histogram, which yields an average current change produced by each detected photon of 0.19 ± 0.01 nA. The half-widths at the $1/e$ points of the $N = 0$, 1 and 2 gaussian peaks are 58 ± 4, 110 ± 10 and 130 ± 30 pA, respectively. These values correspond

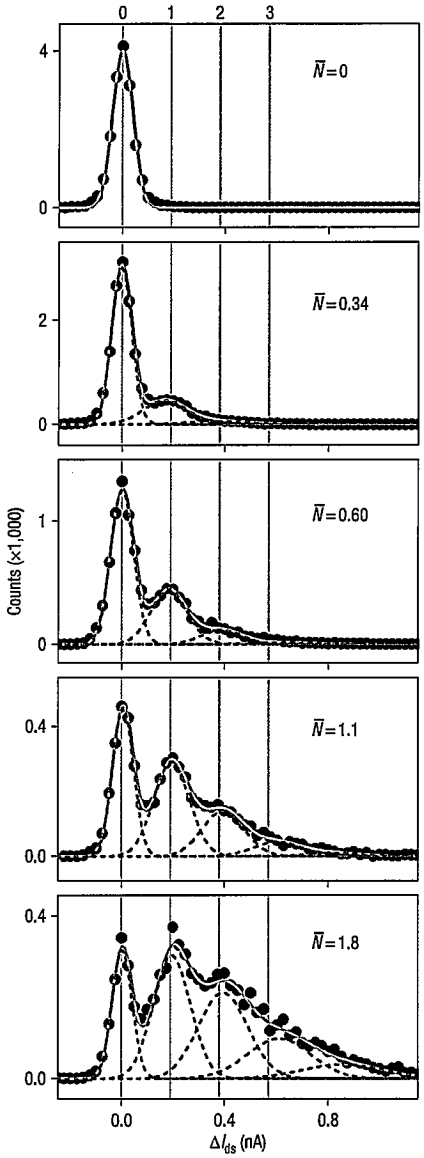

Figure 3 Photon-number discrimination. Histograms of binned current changes, ΔI_{ds}, measured for five different average pulse fluences. Each panel is labelled with the mean number of photons detected per pulse $\bar{N}$. The total number-of-measurements-acquired-for-each-data-set-(from-top-to-bottom)-are 16,591, 16,591, 5,057, 5,609 and 7,485. Grey vertical lines indicate current changes calculated from equation (1) caused by the detection of $N = 0$, 1, 2 and 3 photons. Green curves are Poisson fits to the data, where the detector response is taken into account by assuming gaussian distributions (red dashed curves) for each of the photon number peaks.

to fractional widths of the peak spacings of 0.29 ± 0.02, 0.53 ± 0.05 and 0.64 ± 0.16. Whereas the zero-photon peak is broadened solely by electrical noise, the peaks associated with non-zero number states are expected to be additionally broadened owing to non-uniform contributions of holes trapped in different QDs of the ensemble. The change in I_{ds} caused by N photons is the sum of N single-photon changes in the channel current. Consequently, as long as the signal changes caused by the charging of separate QDs are uncorrelated, the variances of the individual peaks should increase linearly with N. The peak widths extracted from the numerical fits are consistent with such N-dependent broadening.

Table 1 Probabilities of correctly determining the number of detected photons for a given pulse for $\bar{N} = 1.1$.

Photon number	Decision region	Percent correct
0	$\Delta I_{ds} \leq 80$ pA	94
1	80 pA $< \Delta I_{ds} \leq 310$ pA	89
2	310 pA $< \Delta I_{ds} \leq 530$ pA	83
≥ 3	$\Delta I_{ds} > 530$ pA	90

A good figure of merit for the photon-number-resolving detector is the probability of correctly determining the number of photons for a given shot. In the case of an ideal detector with perfect photon-number resolution, photon number states can be unambiguously assigned to precise responses of the detector. In practice, however, uncertainty in the detector's responses to individual photons causes ambiguity in the determination of N. As a result, we must assign a decision region for the current changes associated with each number state. Assigning the decision regions such that the probability of correctly determining N is optimized depends strongly on the response characteristics of the detector as well as the photon-number distribution of the light under study. In Table 1 we list the probabilities of correctly determining N for defined decision regions, given *a priori* knowledge that the incident pulses of light are produced by a Poisson source and that $\bar{N} = 1.1$. The decision regions and the probabilities are determined from the experimental data and the gaussian fits presented in Fig. 3 for $\bar{N} = 1.1$. The decision-region boundaries for each photon number N are defined by the points where the corresponding gaussian function intersects the gaussian functions associated with the preceding and succeeding photon number ($N \pm 1$). We evaluate the probability of accuracy for each number state by dividing the area of the gaussian function contained within the corresponding decision region by the total area of all the gaussian functions contained within that region. The calculated values indicate that we can determine N for each pulse with $\geq 83\%$ confidence. Increased probabilities can be achieved by narrowing the decision regions; however, this produces regions where N is undefined. Counts occurring within these regions must be disregarded, reducing the effective count rate of the measurements.

In conclusion, we have explicitly demonstrated the photon-number-discriminating capabilities of a semiconductor detector that uses self-assembled QDs as optically addressable floating gates in a δ-doped FET. We observe well-defined peaks in histograms of the detector's responses to laser pulses that correspond to the confinement of discrete numbers of photo-generated holes in QDs. The measured responses are in excellent agreement with theory and reflect the Poisson statistics of the laser light. In previous work[12,13], we showed that $68 \pm 18\%$ of the holes excited in the GaAs absorption region are trapped by QDs, representing the internal quantum efficiency of the detector. Consequently, the number of trapped holes represents, to a large degree, the number of photons absorbed in the dedicated absorption layer. The overall detection efficiency (as defined by the fraction of photons incident on the detection area that are counted) is at present limited by the transmission of the semitransparent gate and the absorption of the active GaAs layer. To directly measure the photon-number states of the incident pulses, the incident light needs to be more efficiently coupled to

the dedicated absorption layer. Higher detection efficiencies should be possible by embedding the absorption layer in a resonant cavity. Future studies will also include tailoring the material composition of the detector to enable photodetection at telecommunications wavelengths and investigating the operation of the device at increased speeds. We have shown that QDOGFETs respond to both light and electrical resets on microsecond timescales[13]. Previously, 400 kHz detection rates have been demonstrated for a similar FET-based single-photon detector through use of a cryogenic radiofrequency amplifier[15]. It is reasonable to expect that such cryogenic amplifiers could also be used in conjunction with our detectors.

METHODS

We studied the photo-response of the QDOGFET at 4 K by illuminating the device with a 0.5 Hz train of attenuated laser pulses and by monitoring the change in I_{ds} caused by each pulse. The incident laser pulses (40 μm spot diameter and 1.54 eV photon energy) were tuned above the bandgap of GaAs but below the bandgap of the AlGaAs layers of the structure. The device was electrically reset 500 ms after the arrival of each laser pulse by raising the applied gate bias to +1 V for 10 ms. This flooded the QDs with excess electrons, which discharged the dots by recombining with the trapped holes. In Fig. 2 we show the response of the channel current to a 20-μs laser pulse, where the laser light was attenuated such that only a few photons were absorbed in the GaAs absorption layer per pulse. We observe a persistent step in I_{ds} that coincides with the arrival of the laser pulse and decays little over the 500 ms interval separating the laser pulse and the electrical reset, when the photo-excited holes are stored in QDs. When the QDOGFET is electrically reset, the current spikes and rapidly returns to its pre-illumination value, indicating that the QDs have been discharged. To determine ΔI_{ds} produced by each laser pulse, we averaged $I_{ds}(t)$ over 50-ms intervals leading up to and following a 10-ms gate surrounding the arrival of each pulse and then subtracted the two averaged values.

Received 5 June 2007; accepted 20 August 2007; published 1 October 2007.

References

1. Waks, E., Inoue, K., Oliver, W. D., Diamanti, E. & Yamamoto, Y. High-efficiency photon-number detection for quantum information processing. *IEEE. J. Sel. Top. Quant. Electron.* **9**, 1502–1511 (2003).
2. Rosenberg, D., Lita, A. E., Miller, A. J. & Nam, S. W. Noise-free high-efficiency photon-number-resolving detectors. *Phys. Rev. A* **71**, 61803(R) (2005).
3. Fujiwara, M. & Sasaki, M. Photon-number-resolving detection at a telecommunications wavelength with a charge-integration photon detector. *Opt. Lett.* **31**, 691–693 (2006).
4. Knill, E., Leflamme, R. & Milburn, G. J. A scheme for efficient quantum computation with linear optics. *Nature* **409**, 46–52 (2001).
5. Brassard, G., Lütkenhaus, N., Mor, T. & Sanders, B. C. Limitations on practical quantum cryptography. *Phys. Rev. Lett.* **85**, 1330–1333 (2000).
6. Di Giuseppe, G. *et al.* Direct observation of photon pairs at a single output of a beam-splitter interferometer. *Phys. Rev. A* **68**, 63817 (2003).
7. Waks, E., Diamanti, E., Sanders, B. C., Bartlett, S. D. & Yamamoto, Y. Direct observations of nonclassical photon statistics in parametric down-conversion. *Phys. Rev. Lett.* **92**, 113602 (2004).
8. Waks, E., Sanders, B. C., Diamanti, E. & Yamamoto, Y. Highly nonclassical photon statistics in parametric down-conversion. *Phys. Rev. A* **73**, 33814 (2006).
9. Waks, E., Diamanti, E. & Yamamoto, Y. Generation of photon number states. *New J. Phys.* **8**, 4–8 (2006).
10. Yusa, G. & Sakaki, H. GaAs/n-AlGaAs field-effect transistor with embedded InAs quantum traps and its programmable threshold characteristics. *Electron. Lett.* **32**, 491–493 (1996).
11. Rose, A. *Concepts in Photoconductivity and Allied Problems* Ch. 1 (Interscience, New York, 1963).
12. Rowe, M. A. *et al.* Single-photon detection using a quantum dot optically gated field-effect transistor with high internal quantum efficiency. *Appl. Phys. Lett.* **89**, 253505 (2006).
13. Gansen, E. J. *et al.* Operational analysis of a quantum dot, optically gated, field-effect transistor as a single-photon detector. *IEEE J. Sel. Top. Quant. Electron.* (in the press).
14. Kardynal, B. E. *et al.* Photon number resolving detector based on a quantum dot field effect transistor. *Appl. Phys. Lett.* **90**, 181114 (2007).
15. Kardynal, B. E. *et al.* Low-noise photon counting with a radio-frequency quantum-dot field-effect transistor. *Appl. Phys. Lett.* **84**, 419–421 (2004).

Acknowledgements